DYNAMICS OF A SEMICONDUCTOR LASER UNDER THE INFLUENCE OF MULTI-SECTION FEEDBACK: APPLICATIONS TO CHAOS-BASED COMMUNICATIONS

S. S. Rusu[1,2] and V. Z. Tronciu[2]

[1] Institute of Applied Physics, Academy of Sciences of Moldova, Chisinau, Moldova
[2]Department of Physics, Technical University of Moldova, Chisinau, Republic of Moldova
E-mail: tronciu@mail.utm.md

(Received October 20, 2016)

Abstract

This paper reports the numerical results of the dynamical behavior of a novel integrated semiconductor laser subject to multiple optical feedback loops. Due to the influence of the feedback, under appropriate conditions, the system exhibits a strong chaotic behavior suitable for chaos-based communications. We demonstrate the effect of the relevant device parameters on the laser dynamics and show that the properties of the external cavity and its position in the device have a considerable influence on the chaotic behavior of the laser. The synchronization of two unidirectionally coupled lasers is studied numerically. Finally, we find appropriate conditions for message encoding by a chaos modulation technique using compact lasers under the influence of multiple-feedback loops.

1. Introduction

In the last decade, the phenomena of destabilization and chaos of laser emission by external cavities have been the subject of considerable attention, with the studies mainly motivated by the prospect of the applications to chaos-based communication (CBC) systems. Semiconductor lasers subjected to the influence of optical feedback from a distant mirror have been extensively investigated for the past two decades and different dynamical behaviors have been characterized, including periodic and quasi-periodic pulsations, low-frequency fluctuations, coherent collapse, optical turbulence, and chaos (for more details, see [1]). It is well known that the chaotic waveform is suitable for CBC. Thus, the chaotic communications have become an option to improve privacy and security in date transmission, especially after the recent field demonstration of the metropolitan fiber networks of Athens [2]. In optical CBCs, the chaotic waveform is generated by using semiconductor lasers with either all-optical or electro-optical feedback loops [3–10]. Configurations using Fabry–Perot resonators providing the optical feedback, the so-called frequency selective feedback, have also been considered [11–13]. Several message encoding schemes have been proposed in the literature [14, 15]. Here, we include the message as a modulation in the amplitude of the chaotic carrier (chaos modulation) [3, 11, 12]. The message can be decoded at the receiver by comparing its input with message with its output. The main aim of recent technological progress has been the production of structures with stable properties and the possibility of their application in different areas. The distributed feedback

(DFB) lasers with external feedback from multi sections might be a key element for devices used in the CBC system. Note that the communication method based on chaos would bring great benefits to secure data transmitted in communication networks.

In this paper, we consider an integrated compact device composed of a semiconductor laser subject to the feedback from multiple cavities with the aim of generating a complex chaotic waveform suitable for applications in CBCs. The obtained results show that, under appropriate conditions, DFB lasers with multiple external feedbacks exhibit a chaotic behavior appropriate for CBCs. An advantage of the proposed system compared with that of conventional optical feedback is that the chaotic behavior occurs for short lengths of cavities, which makes more compact device. The paper is structured as follows. We start in Section 2 by describing the laser setup and we introduce an appropriate model to describe the system dynamics. Section 3 presents a study of the dynamics of a laser under the influence of multi cavity feedback. The suitable conditions for the chaotic evolution of the output power system due to the influence of feedback are determined. The synchronization properties of two such devices and the chaos modulation encryption method are also demonstrated. Finally, conclusions are given in Section 4.

2. Laser model and equations

Figure 1a shows the structure of the DFB laser under the influence of feedback from equally distributed external cavities. We consider a single-mode continuous-wave (CW) laser coupled to longitudinal multi-cavities. The first mirror is located at distance L from the laser facet, and the distance between mirrors is taken also L. We consider five external mirrors. At the same time, Fig. 1b shows a sketch of possible experimental implementations of the setup from Fig. 1a with a CW laser with two air gaps, similar to that of [11]. The DFB section is coupled to two phase sections, two optically transparent straight waveguides, and two air gaps. The phase sections were introduced to control the feedback phases of the external cavities by adjusting the small bias current of them. For more details on the fabrication technique, see [11]. Thus, our present investigation has two aims. First, we want to sort out how the dynamics of the laser, especially the chaotic properties of the device, can be tailored by appropriately designing the external cavities similar to that in Fig. 1a. Second, we want to apply chaos modulation technique to a suited experimental structure as in Fig. 1b.

The system dynamics is analyzed in terms of the extended Lang–Kobayashi model [16] for the complex amplitude of electric field E and density of carriers; we consider the approximation of a single loop and neglect the multi-reflections within the cavities:

$$\frac{dE}{d\tau}=\frac{1}{2}(1+i\alpha)\left[\frac{g(N-N_0)}{1+\varepsilon|E|^2}-\frac{1}{\tau_p}\right]E+\sum_{n=1}^{5}\gamma_n\exp\left(-i\sum_{k=1}^{n}\varphi_k\right)E(\tau-n\tau_L)\,, \tag{1}$$

$$\frac{dN}{dt}=\frac{I}{e}-\frac{1}{\tau_e}N-\frac{g\left(N-N_0\right)}{1+\varepsilon|E|^2}|E|^2\,, \tag{2}$$

where γ_n (n = 1–5) are the feedback strengths governed by the reflectivity's R_n. Other parameters are as follows: Henry factor of α = 5, differential gain coefficient of $g = 1.5\cdot10^{-5}$ ps^{-1}, and saturation of the gain coefficient of $\varepsilon = 5\cdot10^{-7}$. The lifetime of photons and carriers are $\tau_p = 3\cdot10^{-3}$ ps and τ_e = 2 ns, respectively. These parameter values are used for the calculated results that are shown in all figures of the paper.

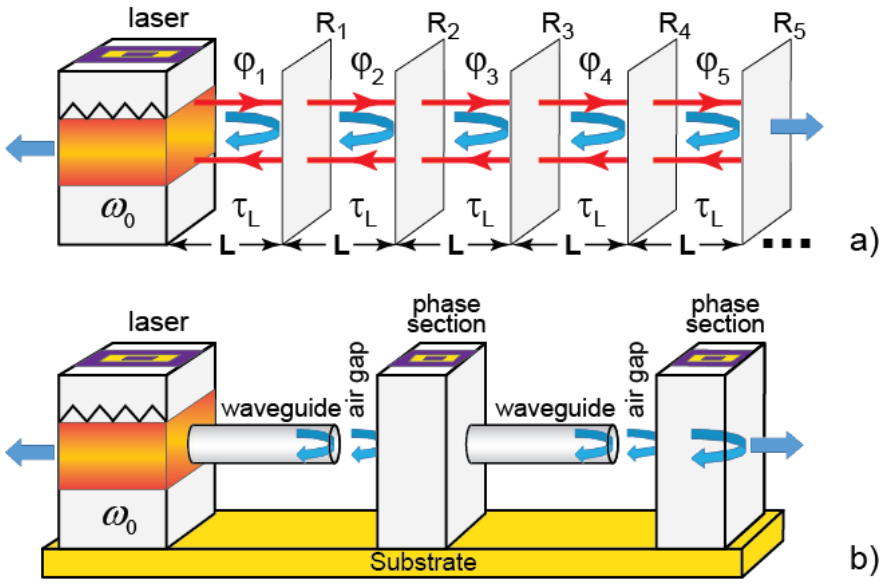

Fig. 1. (a) Sketch of a setup for chaos synchronization and message encoding using semiconductor lasers under the influence of multiple cavity feedback and (b) view of practical implementation of the proposed integrated device with double air gaps. The length of the air gap sections is 5 μm, similar to that of a single air gap device used in [11]. The reflection between air gaps and both waveguide and phase sections is ~30%. The setup is not in scale.

3. Results and discussion

We begin by considering a more general case of optical feedback originated from multi section cavities shown in Fig. 1a. We examined the dynamics of a semiconductor laser with optical feedback from multi section cavities using equations (1)–(2). It is well known that, for small feedback strength, a laser shows either CW or pulsating operations non-applicable in CBC systems. Chaotic behavior appears as the feedback strength is increased enough. Thus, an increase in feedback strength leads to the appearance of chaotic behavior in the system. Figure 2 shows numerical calculations of the time evolution of output power and phase portrait and the power spectrum of the semiconductor laser under the influence of optical feedback from multi cavity in the chaotic regime appropriate for chaos based communications for different feedback strength. Thus, feedback strength γ ($\gamma = \gamma_1 = \gamma_2 = \gamma_3 = \gamma_4 = \gamma_5$) and phase φ ($\varphi = \varphi_1 = \varphi_2 = \varphi_3 = \varphi_4 = \varphi_5$) are considered as main bifurcation parameters. The feedback strengths are governed by the cavity reflectivity's. It is shown in Fig. 2a that, for $\gamma = 10$ ns^{-1} the output power describes a quasi-chaotic behavior and the phase portrait is a distorted limit cycle. In the power spectrum, a few harmonics are dominant. For $\gamma = 15$ ns^{-1} the time evolution of output power and the phase portrait become more complicated and new harmonics appear in the power spectra as shown in Fig. 2b. Thus, an increase in the level of optical feedback strength triggers certain trajectories to chaos. One can see in Fig. 2c that the oscillations of the output

power become more complicated and chaotic behavior appears and the phase portrait is a strange attractor. Thus, due to the influence of multiple feedbacks, the laser behavior has been found to be chaotic for a large range of parameters and laser bias currents.

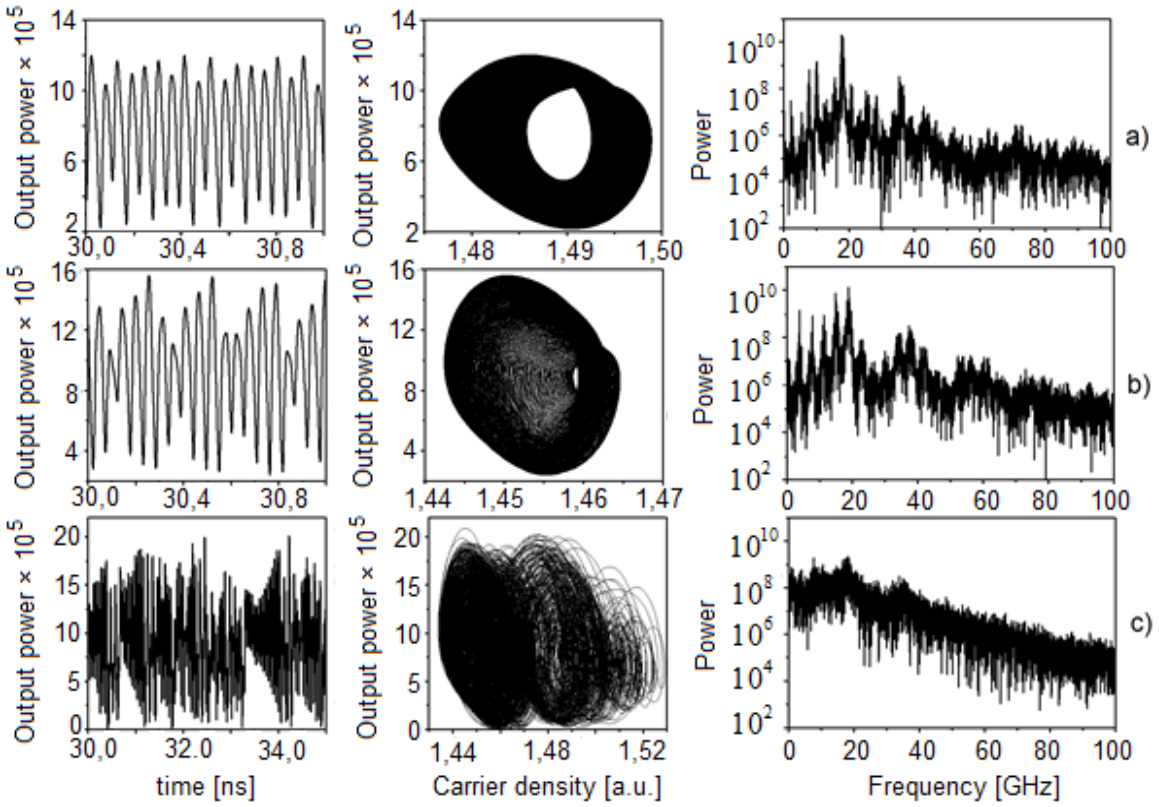

Fig. 2. Pulse trace of output power (left), phase portrait (center), and power spectrum (right) of a semiconductor laser under the influence of optical feedback from multi cavity for the chaotic behavior: (a) $\gamma = 10$ ns^{-1} – quasi-chaos, $\gamma = 15$ ns^{-1} – chaos, and $\gamma = 20$ ns^{-1} – strong-chaos.

Next, we examine the laser dynamics in terms of bifurcation diagrams. A typical calculation of bifurcation is shown in Fig 3a, where the feedback strength is the bifurcation parameter. One can see an evident strong chaotic behavior for $\gamma > 14$. If we increase the injected current, the CW operation is observed (see Fig. 3). Then the laser begins to produce pulsations (*P*) through a Hopf bifurcation (*H*) marked by a circle in Fig. 3a. One can observe the appearance of a low-amplitude chaotic behavior for low feedback strengths followed by the CW operation and a scenario compatible with the quasi-periodic route to chaos. As the feedback strength further increases, a second scenario compatible with the quasi-periodic route to chaos appears. For large values of the feedback strength, the system displays a chaotic behavior. If φ is considered as a bifurcation parameter, the chaotic behavior is present for all values of phase φ (see Fig. 3). Thus,

the proposed setup can generate the fully chaotic pulse traces suitable for chaos based communications.

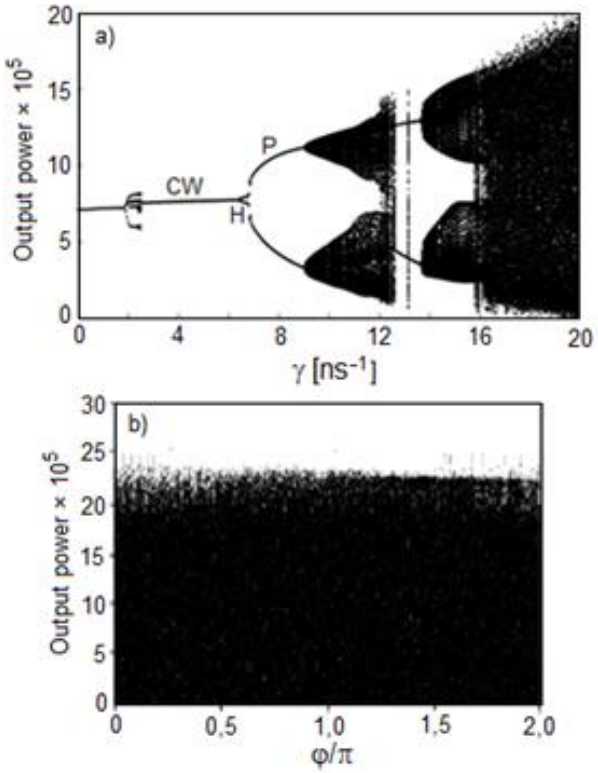

Fig. 3. Bifurcation diagram for (a) γ being a bifurcation parameter and phase $\varphi = \pi/2$ and (b) φ bifurcation parameter and $\gamma = 20$ ns^{-1}.

It is well known that the autocorrelation time is related to the complexity of the generated chaos. Figure 4 shows the calculated autocorrelation time [17] of a semiconductor laser under the influence of optical feedback from multi cavity in two parameters plane phase. The white region corresponds to CW or periodic regimes. The red region shows the strong chaos regime with autocorrelation time $\tau_c < 100$ ps. It can be clearly seen how the autocorrelation time changes and, in particular, how the autocorrelation time becomes much shorter for specific feedback strength and phases providing more secure conditions for chaos-based communications. Thus, as the feedback strength increases, the autocorrelation time decreases, being an indication that the laser dynamics becomes more chaotic.

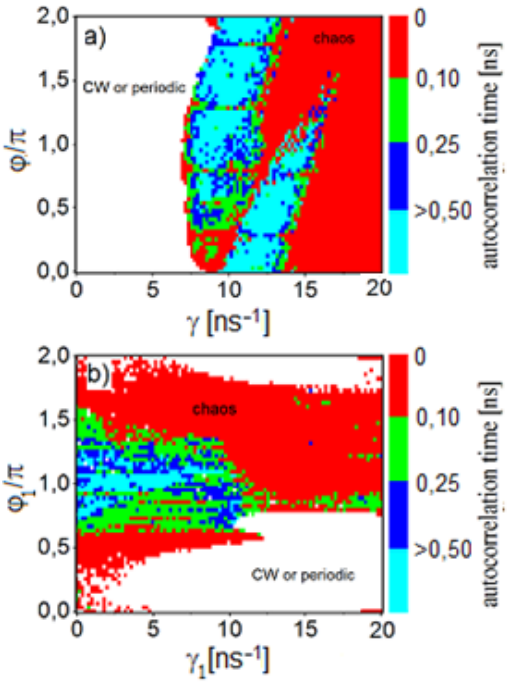

Fig. 4. Autocorrelation time in the plane of different parameters: (a) plane ($\varphi - \gamma$) and (b) plane ($\varphi_1 - \gamma_1$) for $\varphi_2 = \pi/2$, $\varphi_3 = \pi/4$, $\varphi_4 = \pi$, $\varphi_5 = 3\pi/2$, and $\gamma_2 = 5$, $\gamma_3 = 10$, $\gamma_4 = 15$, $\gamma_5 = 20$.

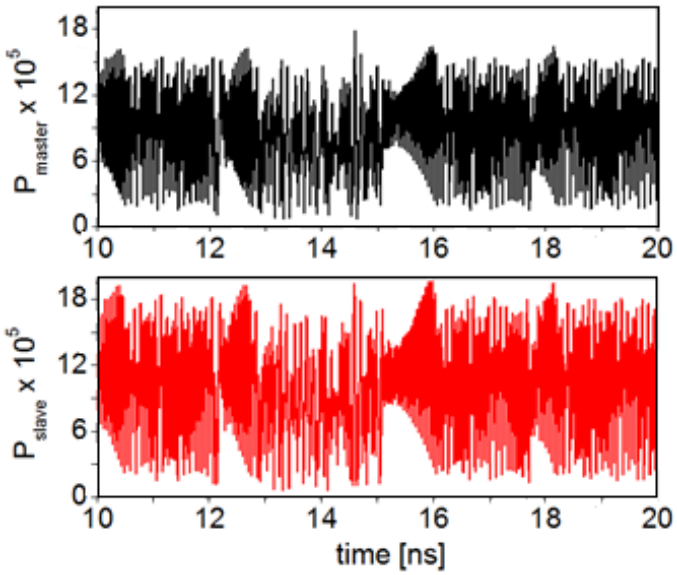

Fig. 5. Synchronization process of two lasers for $k = 90$. Pulse traces of master (top) and slave (bottom) lasers showing a chaotic behavior. Other parameters: $\gamma = 15$ ns^{-1}, $\varphi = 3\pi/4$.

So far, we have discussed different aspects of the transmitter laser dynamics under the influence of multiple feedbacks. In what follows, we focus on the transmitter–receiver configuration, evaluate the synchronization properties, and make use of these integrated devices for message encoding and decoding in CBCs. In the chaos modulation technique, the message is encoded as a small amplitude modulation of the emitted field of the master [11]. At the receiver system, the message is decoded by making the difference between the input of the receiver with its output, which is ideally synchronized to the carrier. Thus, in what follows, we numerically analyze the synchronization properties of two lasers connected in unidirectional direction. It is well known that the synchronization can be quantified by measuring the cross-correlation coefficient. Figure 5 shows the chaotic behavior of master (top) and slave (bottom) lasers in the process of synchronization under the influence of optical feedback from multi cavity. It can be clearly seen that the two time traces remain similar to each other.

Figure 6 shows the emitted power of the slave laser versus the power of the master (synchronization diagram) for feedback strength $\gamma = 15$ ns^{-1} and different levels of coupling parameter k. If the coupling parameter is equal to zero, as shown in Fig. 6a, the trajectories of the master and slave lasers depart from each other and the synchronization map is a cloud of points showing the lack of correlation between outputs. With an increase in the coupling parameter to $k = 50$ ns^{-1}, the synchronization map shows a week synchronization process (see Fig. 6b). By increasing the coupling to $k = 75$ ns^{-1}, the synchronization improves. With a further increase in coupling to 90 ns^{-1}, the synchronization becomes clear and cross correlation coefficient approaches unity (see Fig. 6d).

Figure 7 shows the map of synchronization quality in the plane of different parameters for coupling coefficient fixed to $k = 90$ ns^{-1}. Figure 7a displays the value of the correlation function in the parameter space ($\varphi - \gamma$). High degree of synchronization is characterized by green color. It can be clearly seen that the region of high correlation coefficients is wide. This conclusion is confirmed also by Fig. 7b, where the region with a low cross correlation coefficient is very narrow and present only for certain phases. However, note that the higher cross correlation region includes also the CW and self-pulsation regimes. Thus, in order to choose an appropriate initial point for message encoding in the chaos modulation technique, we have to select a certain point operating in the chaotic regime from Fig. 5.

Further on, we study the transmission–reception configuration of two lasers shown in Fig. 1b connected in unidirectional configuration [11]. We examine the encrypting and decrypting of a digital message in the chaos modulation technique. Figure 8 illustrates the process of transmission of a 10 Gb/s digital signal. Panel (a) shows the shape of the incident signal, i.e., the one that should be sent. Panels (b) and (c) show the output power of the master laser without a message and with it, respectively. Panel (d) shows the decoded message, as indicated in [11], and filtered by an appropriate low-pass filter [18]. This figure shows that, for the case where the parameters of both lasers coincide, the message is fully recovered. Thus, we have theoretically shown that the chaotic modulation method can be implemented in a setup of lasers under the influence of multiple optical feedbacks.

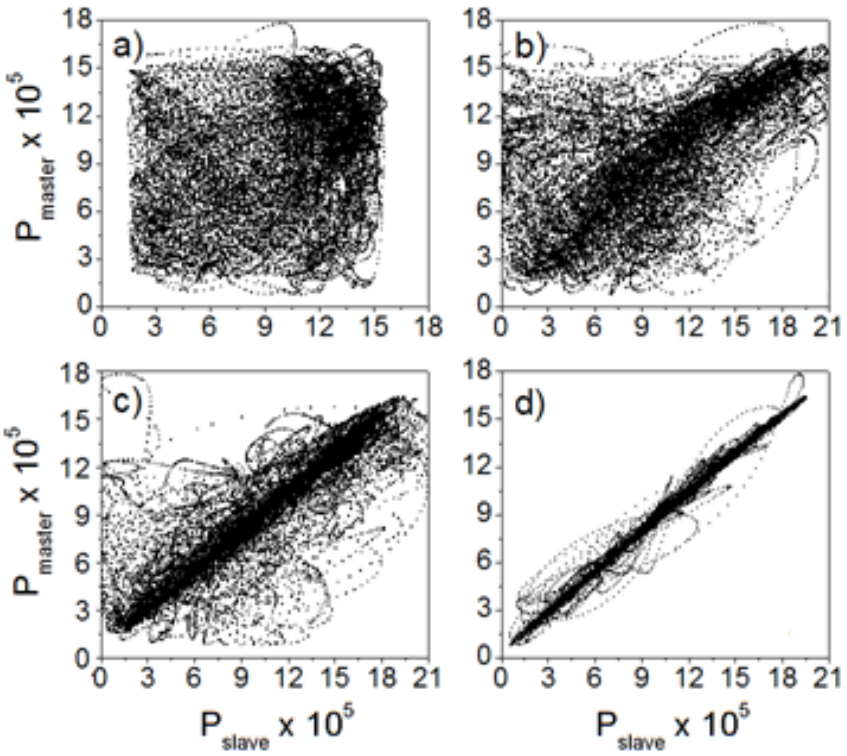

Fig. 6. Synchronization diagrams for different levels of the coupling parameter: (a) $k = 0$ ns^{-1}, (b) $k = 50$ ns^{-1}, (c) $k = 75$ ns^{-1}, and (d) $k = 90$ ns^{-1}. Other parameters: $\varphi = 3\pi/4$, $\gamma = 15$ ns^{-1}.

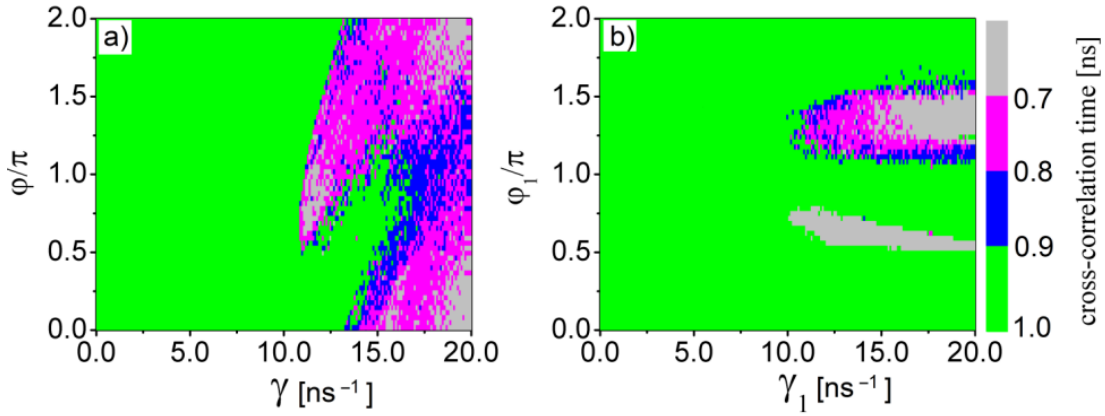

Fig. 7. Cross-correlation time in the plane: a) $(\varphi - \gamma)$, b) $(\varphi_1 - \gamma_1)$ for $\varphi_2 = \pi/2$, $\varphi_3 = \pi/4$, $\varphi_4 = \pi$, $\varphi_5 = 3\pi/2$, and $\gamma_2 = 5$ ns^{-1}, $\gamma_3 =$ ns^{-1}, $\gamma_4 = 15$ ns^{-1}, $\gamma_5 = 20$ ns^{-1}.

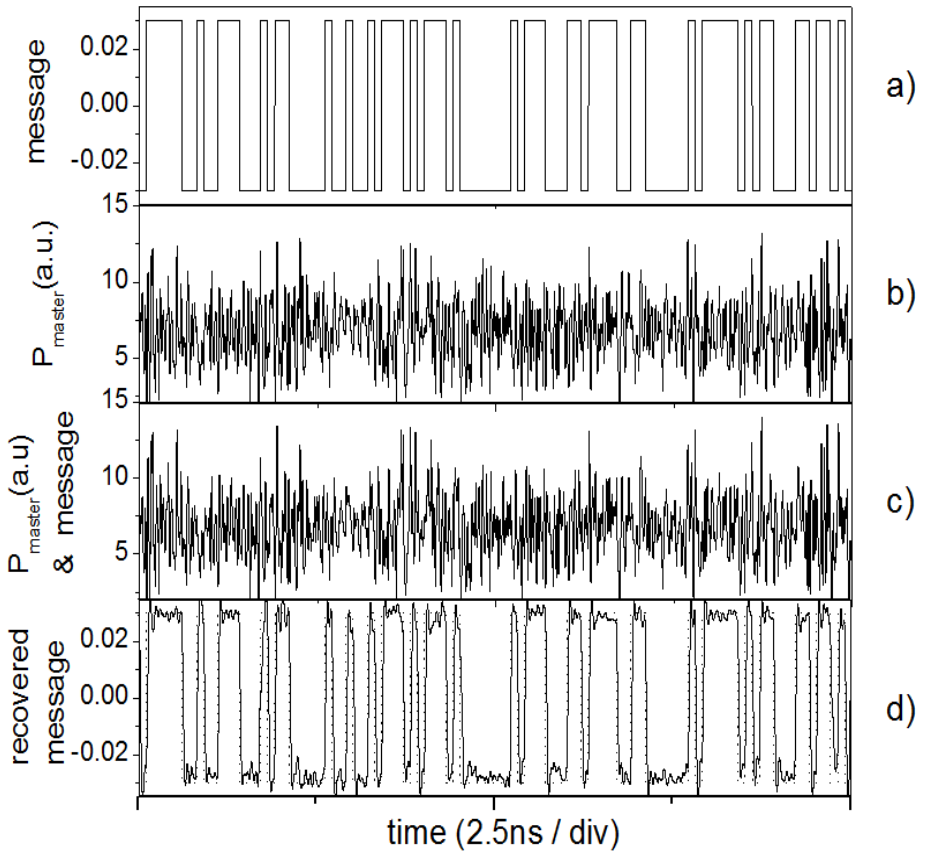

Fig. 8. Numerical results of encoding and decoding of a 10 Gbit/s digital message using chaos modulation technique in the master and slave lasers configurations shown in Figure 1b). a) Encoded message. b) Output of the master laser without message. c) Transmitted signal (with message) d) Decoded message and recovered message after filtering (solid line) and input message (dotted line). Other parameters: length of waveguide – 5 mm, length of airgap 5 μm, length of phase section 200 μm, $\varphi = \pi/2$, $k = 50$ ns^{-1}.

4. Conclusions

In terms of the Lang–Kobayashi equations, the dynamics of a single mode semiconductor laser with optical feedback that comes from multi cavities has been investigated. A novel setup for the realization of multiple feedbacks has been proposed. The presence of several external cavities results in a more complex system oscillations keeping the device compact. Thus, an advantage of the proposed system compared with that of conventional optical feedback is that a chaotic behavior appropriate for CBC occurs for short lengths of cavities. We have shown that two of these devices with identical parameters can be synchronized when operating in a chaotic regime in a master–slave configuration. It has been shown that, for the parameter values where synchronization with higher cross correlation is achieved, it is possible to encode a higher bit rate message in the carrier using the chaos modulation technique. Finally, the message can be

appropriately recovered. We believe that our work provides a good basis for future studies and, in particular, provides some pointers for more detailed investigations of compact lasers with feedback from external multi-section cavities and their applications for CBC.

Acknowledgments. The authors acknowledge the support of projects STCU -5993, 14.02.116F and the technical support from A. Sanduta. VZT acknowledges the support from the Alexander von Humboldt Foundation and from CIM–Returning Experts Programme.

References

[1] B. Krauskopf, and D. Lenstra, (Eds.): Fundamental Issues of Nonlinear Laser Dynamics. AIP Conf. Proc. 548, (2000).
[2] A. Argyris, D. Syvridis, L. Larger, V. Annovazzi-Lodi, P. Colet, I. Fischer, J. García-Ojalvo, C. R. Mirasso, L. Pesquera, and A. L. Shore, Nature 438, 343, (2005).
[3] C. R. Mirasso, P. Colet, and P. Garcia-Fernandez, IEEE Photon. Technol. Lett. 8, 299, (1996).
[4] V. Annovazzi-Lodi, S. Donati, and A. Scire, IEEE J. Quantum Electron. 32, 953, (1996).
[5] S. Sivaprakasam, and K. A. Shore, Opt. Lett. 24, 466, (1999).
[6] I. Fischer, Y. Liu, and P. Davis, Phys. Rev. A 62, 011801(1), (2000).
[7] A. Bogris, D. F. Kanakidis,. A. Argyris, and D. Syvridis, IEEE J. Quantum Electron. 40, 1326,(2004).
[8] S. Tang, and J. M. Liu, Opt. Lett. 26, 596, (2001).
[9] N. Gastaud, S. Poinsot, L. Larger, J. M. Merolla, M. Hanna, J. P. Goedgebuer, and E. Malassenet, Electron. Lett. 40, 898, (2004).
[10] F. Y. Lin,. and M. C. Tsai, Opt. Express 15, 302, (2007).
[11] V. Z. Tronciu, C. Mirasso, P. Colet, M. Hamacher, M. Benedetti, V. Vercesi, and V. Annovazzi-Lodi, IEEE J. Quantum Electron. 46, 1840, (2010).
[12] V. Z. Tronciu, C. Mirasso, and P. Colet, J. Phys. B: At. Mol. Opt. Phys. 41, 155401, (2008).
[13] V. Z. Tronciu, I.V. Ermakov, P. Colet, and C. Mirasso, Opt. Commun. 281, 4747, (2008).
[14] J. Ohtsubo, IEEE J. Quantum Electron. 38, 1141, (2002).
[15] G.D. VanWiggeren, and R. Roy Science 279, 1198, (1998).
[16] R. Lang, and K. Kobayashi, IEEE J. Quantum Electron. 16, 347, (1980).
[17] T. Perez, M. Radziunas, H.-J. Wünsche, C.R. Mirasso, and F. Henneberger, IEEE Photonics Technol. Lett. 18, 2135, (2006).
[18] A. Sanchez-Diaz, C. Mirasso, P. Colet, and P. Garcia-Fernandez, IEEE J. Quantum Electron. 35, 292, (1999).